UDC 532.528

SOME WAYS OF HYDRODYNAMIC FIN APPLICATION FOR UNDERWATER SUPERCAVITATING VEHICLES

V. N. Semenenko†, O. I. Naumova

Institute of Hydromechanics of NAS of Ukraine
Zhelyabov Str., 8/4, 03057, Kyiv, Ukraine
†E-mail: vnsvns60@gmail.com

Received 25.09.2017

The paper deals with considering the two non-traditional ways of application of hydrodynamic fins for high-speed underwater supercavitating vehicles. The techniques for active roll stabilization and course control of the moving supercavitating vehicle are developed that use the regulation of the roll angle by means of both the special roll fin, and the automatic error-closing control system. The examples of a computer simulation of the course of maneuvering of the supercavitating vehicle controlled with the vertical hydrodynamic fins having zero roll angle stabilization are given along with the cases of the roll angle regulation. A method for determining the equilibrium motion parameters (balancing) of the supercavitating vehicle is developed for the case when a pair of identical horizontal cavity-piercing fins is used for complete or partial compensation of the vehicle's weight. The examples of a computer simulation of the motion of the supercavitating vehicle with horizontal fins in both the planing avoidance mode, and the combined mode are presented. It is shown that the steady-state longitudinal motion of the balanced supercavitating vehicle in the planing avoidance mode is stable "in the small", in contrast to its motion with planing in the cavity. It is found that, the horizontal fins in the combined motion mode can play a damping role suppressing the supercavitating vehicle motion instability "in the small", however, after a long time interval, the motion loses the global stability. The computer simulation suggests that the activation of the automatic depth stabilization makes the supercavitating vehicle motion stable in general in all the examined cases. Also it is revealed that course maneuverability of the supercavitating vehicle controlled with the vertical fins is maximal when starting the balancing in planing avoidance mode, but it deteriorates dramatically when starting the balancing in the combined mode.

KEY WORDS: supercavitating vehicle, control, maneuvering, fins, roll, computer simulation

1. INTRODUCTION

A natural way to attain a very high speed in water is to form the motion in the supercavitation regime, when a cavity filled by water vapour or gas is formed around a body with the

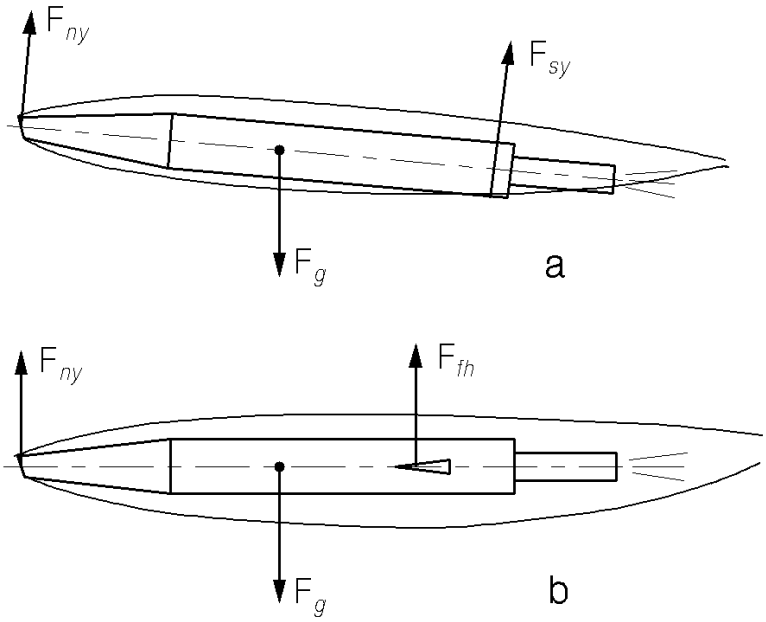

Fig. 1. Two modes of a SC-vehicle motion:
a — planing in a cavity mode, *b* — planing avoidance mode

help of a special nose cavitator [1]. In this case the water drag to the motion is dramatically decreased due to minimization of both the friction drag and the base drag.

The regime of motion of a supercavitating vehicle (briefly a SC-vehicle) is traditional, when the vehicle is planing by its small tail part along the lower cavity wall (the planing in a cavity mode, see Fig. 1a). In this case the vehicle weight F_g is compensated by the hydrodynamic lift on the wetted body part F_{sy}, and an arising moment relatively to the vehicle mass center is compensated by the moment of the lift F_{ny} created by the cavitator inclination.

The SC-vehicle dynamics is very complex due to the nonstationary behavior of the cavity and the complex discontinuous interaction of the body with the cavity walls. In particular, the steady-state longitudinal motion of the SC-vehicle in the planing in a cavity mode is unstable on depth, therefore there is a necessity of active depth stabilization of the SC-vehicle motion. In practice, the depth stabilization of the SC-vehicle motion is realized by the automatic error-closing regulation of the cavitator inclination angle δ_z (δ-stabilization) [2]. The second problem is choosing an optimal strategy of control of the SC-vehicle motion, that ensures specified parameters of its course maneuverability [3, 4].

In our works [5–8], the comparative analysis of the following three methods of the SC-vehicle motion control was given:

1) inclination of the cavitator with two degrees of freedom (δ-control);

2) deflection of the propulsor thrust vector with two degree of freedom (η-control);

3) using vertical and horizontal hydrodynamic cavity-piercing fins (f-control).

In this case we supposed that the SC-vehicle moves in the traditional planing in a cavity mode (see Fig. 1a). The obtained conclusions are briefly listed in Section 3.

The paper [9] considers an alternative scheme of the SC-vehicle motion avoiding the planing of the vehicle tail part along the cavity wall, which results in instability of the SC-vehicle motion (the planing avoidance mode). In this case a pair of horizontal cavity-piercing fins located in the vehicle tail part are used to compensate the vehicle weight F_g (see Fig. 1b). The work [10] is based on a similar idea, in this case the weight compensation and stability of the SC-vehicle longitudinal motion is ensured by means of an ring-type tail wing. The work [11] considers a possibility of maintenance of the planing avoidance mode by regulating the gas supply into a ventilated cavity.

Use of hydrodynamic fins as operation controls of the SC-vehicle motion, which serve directly to create transversal control forces (as in [4, 8]), may be considered as traditional. This article considers two non-traditional ways of application of hydrodynamic fins for SC-vehicles.

A method of active roll stabilization of the SC-vehicle and a method of course control of the SC-vehicle motion by regulating the roll angle θ (θ-control, which is analogous to the "bank-to-turn" control) are investigated in Sections 4 and 5. Examples of computer simulation of course maneuvering of the SC-vehicles at both the f-control with the zero roll angle θ-stabilization, and the θ-control are given.

A method for determination of the balanced values of the motion parameters (balancing) of the SC-vehicle with horizontal fins in the planing avoidance mode (see Fig. 1b) and in the combined mode, i. e., if both the horizontal fins and planing of the vehicle body in a cavity are presented, is considered in Section 6. Examples of computer simulation of motion of the SC-vehicle balanced in both the planing avoidance mode and the combined mode are given in Section 7.

2. CALCULATION METHOD AND DESIGN MODEL

For computer simulation of dynamics of the self-propelled guided underwater SC-vehicles with ventilated supercavities we use the approximation mathematical model of 3D motion of supercavitating bodies based on the principle of independence of the unsteady cavity section expansion by G. V. Logvinovich [1]. It includes the following equations and relations:

- – equations of 3D-dynamics of a solid body with six degrees of freedom in the body coordinates;
- equations for calculation of an unsteady cavity shape and its location in the flow coordinates with taking into account the cavity distortions caused by both the cavitator inclination and the gravity effect [12, 13];
- equations for pressure in a ventilated cavity $p_c(t)$, which is determined by a difference between a rate of gas supply into the cavity and a rate of gas loss from the cavity [13,14];
- relations connecting the acting hydrodynamic forces and moments in the body coordinates with the current body and cavity parameters, where the force components when the vehicle is planing in a cavity are calculated by E. V. Paryshev's formulae [7, 15]; to calculate forces on the fins and dimensions of cavities forming past the fins, we use

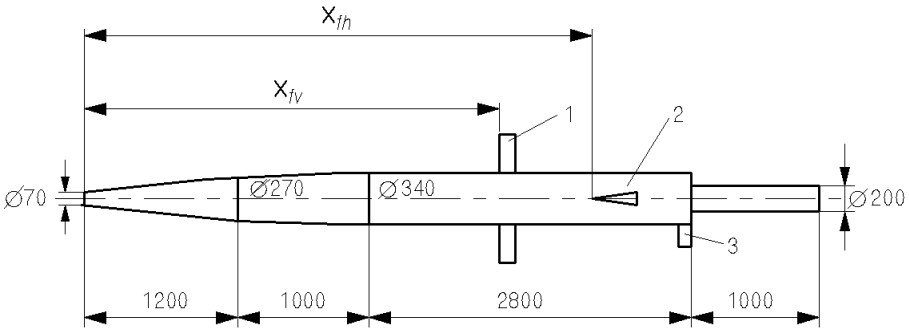

Fig. 2. Sketch of the SC-vehicle design model

the known relations of the linear theory of the supercavitating hydrofoils with a small aspect ratio [8].

All the calculations were performed for the SC-vehicle design model, which is shown in Fig. 2. Its main parameters are the following: the length $L = 6.0$ m, the cylindrical part diameter $D_b = 340$ mm, the cavitator diameter $D_n = 70$ mm, the mass $m = 600$ kg, the mass center position $x_c = 3.0$ m, the moments of inertia relatively to the model axes $I_x = 8.0$ kg·m^2, $I_y = I_z = 900$ kg·m^2. The vehicle has the aft tube with the length 1.0 m and diameter 200 mm, where a nozzle of a rocket or hydrojet engine is located in practice.

The starting parameters of the model motion in the cruise phase are the following: velocity $V = 120$ m/s, depth $H = 10$ m. In this case the cavitation number is $\sigma = 0.02$, the cavity length is $L_c = 6.565$ m, the volumetric gas supply rate into the cavity is $\dot{Q}_{in} = 72.125$ l/s. The balanced values of the parameters in the model without fins steady-state motion in the planing in a cavity mode are the following: the cavitator inclination angle $\delta_z = -5.774°$, the pitch angle $\psi = 0.371°$, the propulsor thrust $F_{pr} = 23.219$ kN.

The model may have a pair of identical vertical fins *1*, pair of identical horizontal fins *2*, and the bottom roll fin *3*. All the fins have a rectilinear shape in plan and a wedge shape in cross section (see Fig. 3). Here, c_f is the fin chord; h_f is the fin span; β_f is the wedge semiangle in the fin section; δ_f is the fin deflection angle; α_f is the fin effective angle of attack. Axes of both the flow coordinates $Ox_0y_0z_0$ and the body coordinates $Ox_1y_1z_1$ are shown in Fig. 3 for the vertical fin case. Real position and dimensions of the fins are given in Table 1.

The vertical fins *1* are intended for the SC-vehicle course maneuvering by deflection on the angle δ_{fv} (see Fig. 3). The horizontal fins *2* are intended for balancing the SC-vehicle by deflection on the angle δ_{fh}. The roll fin *3* is intended for regulating the vehicle roll angle θ by deflection on the angle δ_{fb}.

3. FEATURES OF CONTROL OF SC-VEHICLE MOTION

A course maneuverability of an underwater vehicle is its ability to move with a specified radius of a turning circle r in the horizontal plane. A simple analysis shows that the high-speed SC-vehicles can turn with a minimal radius being $(2 \dots 3)$ orders larger than in the continuous flow, because surfaces of the vehicle contact with water are small [5]. As was

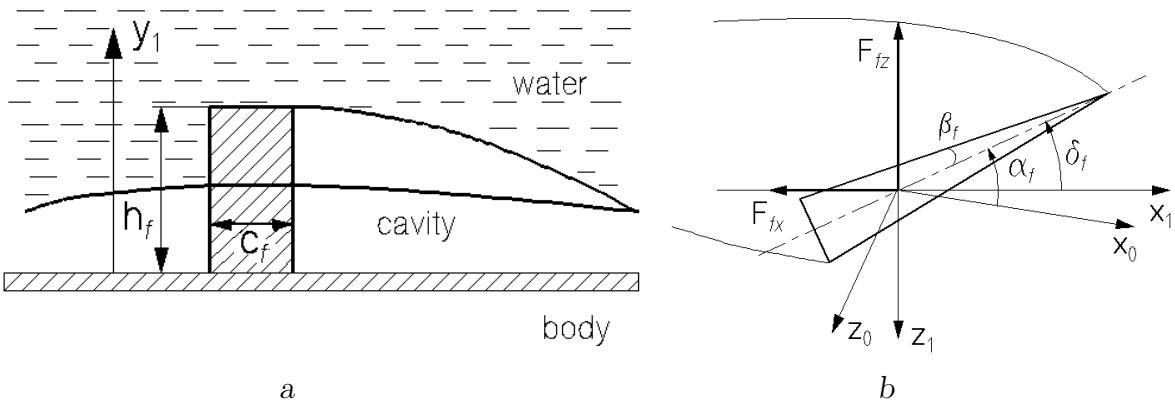

Fig. 3. Scheme of the SC-vehicle fin:
a — side view, b — cross section

Table 1. Position and dimensions of the design model fins

Fins	x_f, m	c_f, mm	h_f, mm	β_f,°
horizontal	4.80	100.0	130.0	3.0
vertical	2.30	100.0	130.0	3.0
roll fin	4.94	50.0	80.0	3.0

shown in work [16], possibility of the SC-vehicle course maneuvering is additionally limited owing to the cavity deformation and, as a consequence, the vehicle wetting. A simple method of estimation of the minimal radius of a turning circle for the SC-vehicle with a disk cavitator is given in [16].

The analysis has shown that the most effective operating control for the SC-vehicle motion is the cavitator (δ-control). However, the δ-control is often insufficient to attain admissible according to [16] radii of a turning circle, because the cavitator inclination angle is limited by a some maximal value δ_{max}. In addition, the cavitator is usually used as an operating control of an automatic system of the motion depth stabilization [2,6]. Therefore, in practice one has to use the hydrodynamic cavity-piercing fins (f-control) for the SC-vehicle course maneuvering.

The SC-vehicle maneuvering with the help of f-control is associated with a significant increase in the motion drag. In the case of high-speed SC-vehicles, the cavity-piercing fins are flown in the supercavitation regime. In this case the efficiency of such an operating control is decreased in comparison with the case of the continuous flow. In addition, the stepwise changing the transversal forces accompanied by a hysteresis effect may occur when varying the fin effective angle of attack α_f (see [17]).

Since the transversal forces on fins of each pair are usually different owing to the cavity asymmetry, the total axial moment arises:

$$M_{fx} = F_{v2}y_{v2} - F_{v1}y_{v1} + F_{h2}z_h - F_{h1}z_{h1}, \tag{1}$$

where y_{v1}, y_{v2}, z_{h1}, z_{h2} are distances from the points of the transversal force application (F_{v1}, F_{v2} on the vertical fins, F_{h1}, F_{h2} on the horizontal fins, respectively) up to the vehicle

longitudinal axis. Here, index 1 is related to both the lower vertical fin and the left horizontal fin, index 2 is related to both the upper vertical fin and the right horizontal fin. The moment M_{fx} leads to increasing the vehicle roll angle θ and, hence, to unfavorable changing the control force direction. Indeed, the horizontal projections of the forces acting on the vertical fins are decreased with increasing the roll angle. Hence, the f-controlled SC-vehicle motion must be stabilized not only on depth, but on the roll as well.

It was shown in work [8] that the frontal location of the vertical fins (the "duck" scheme) is the most effective for the SC-vehicle course maneuvering. When displacing the vertical fins to the aft, their efficiency is decreased approximately by a linear law. The traditional for surface ships and submarines aft location of fins is unacceptable for the SC-vehicle course maneuvering.

The method of η-control by deflection of the propulsor thrust vector is commonly used in aviation and rocketry. But as applied to the SC-vehicle motion η-control is equivalent to the f-control with the aft fins from a hydrodynamic point of view, i. e., it is unacceptable.

4. ROLL STABILIZATION OF SC-VEHICLE MOTION

As was said above, the roll stabilization must be ensured when the f-controlled SC-vehicle course maneuvering. The SC-vehicle roll stabilization may be realized by both the passive methods and the active methods. The passive hydrostatic stabilization of the zero roll angle is realized if the vehicle has the metacentric height (as for surface ships and submarines). The metacentric height h_M is a distance between a center of the vehicle cross section and of the vehicle mass center. If the vehicle mass center is lower than the cross section center on the value h_M, then the restoring moment relatively to the vehicle longitudinal axis occurs with the vehicle roll on the angle θ:

$$M_{gx} = -h_M mg \cos\psi \sin\theta, \tag{2}$$

where ψ is the model pitch angle. As a result, the vehicle will make low-frequency oscillation on roll about the value $\theta = 0$ during motion. In other words, the vehicle is statically stable relatively perturbations of the zero roll angle when $h_M > 0$.

In practice, as applied to the SC-vehicles, the efficiency of the passive hydrostatic roll stabilization is limited because the really achievable values of h_M are small. A method of the passive hydrodynamic roll stabilization with the help of a V-shaped system of cavity-piercing fins is known as well [18]. The fin parameters are selected in such a way that the fins create a total restoring axial moment with the vehicle roll.

We propose a method of active hydrodynamic stabilization of the specified roll angle of the SC-vehicle with the help of a special roll fin. The roll fin *3* is located in the vehicle bottom tail part in the zone of the vehicle planing along the lower cavity wall (see Fig. 2). Dimensions of the roll fin may be essentially smaller than dimensions of the vertical fin *1*, because it serves not to create the transversal force, as at the f-control, but only to create an axial moment. The law for the automatic system of error-closing regulating the angle of the roll fin deflection δ_{fb} for maintenance of the roll angle $\theta = \theta_2$ is set in the form of the "plain autopilot" [2]:

$$\delta_{fb}(t) = -u_1[\theta(t - t_1) - \theta_2] - u_2\omega_x(t - t_1), \tag{3}$$

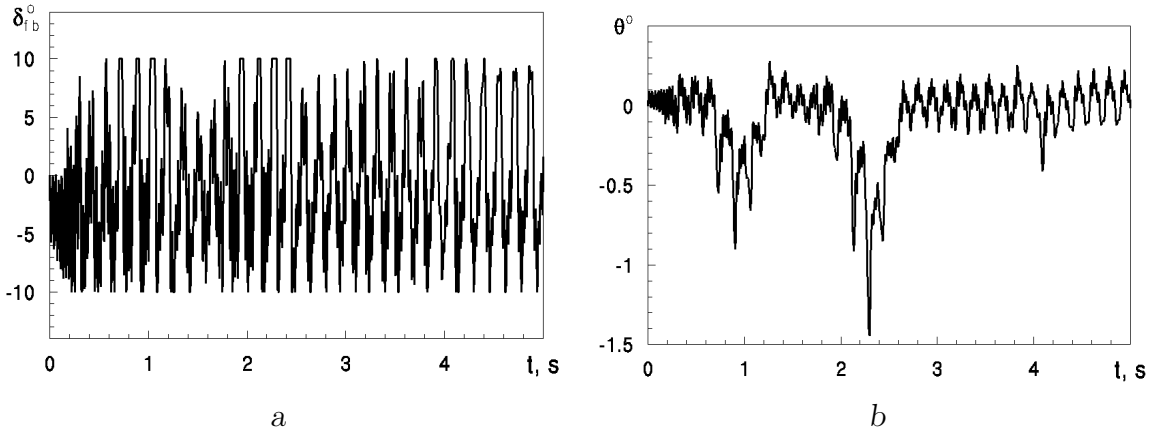

a *b*

Fig. 4. Operation of the automatic system of the zero roll angle stabilization:
a — dependence $\delta_{fb}(t)$, *b* — dependence $\theta(t)$

where $u_1 \geq 0$, $u_2 \geq 0$ are the feedback coefficients (transfer ratios); t_1 is the lag time of the actuator operation; ω_x is the angular velocity relatively to the vehicle longitudinal axis. In this case the design restriction for varying the roll fin deflection angle has to been introduced:

$$|\delta_{fb}(t)| \leq \delta_{fb1}, \qquad t > t_{beg}, \tag{4}$$

where $t = t_{beg}$ is time of beginning of the θ-stabilization system operation.

Fig. 4 shows an example of operation of the automatic system of stabilizing the zero roll angle at computer simulation of the f-controlled SC-vehicle course maneuvering. Graphs of varying the roll fin deflection angle δ_{fb} (Fig. 4a) and corresponding attained magnitudes of the roll angles θ (Fig. 4b) on the starting interval $0 < t < 5.0$ s are given in Fig. 4. The calculations were performed for the following control parameters: $\delta_{fv} = 5.0°$, $u_1 = 0.1$, $u_2 = 0.3$, $\delta_{fb1} = 10.0°$.

As can be seen, both the functions $\delta_{fb}(t)$ and $\theta(t)$ take the form of steady quasiperiodic oscillation with the fundamental frequency 6.80 Hz on completion of the transient process. In this eample, the following maneuver parameters were attained: $\dot{\chi} = 7.645°/\text{s}$, $r = 0.888$ km. Here $\dot{\chi}$ is the speed of varying the path angle $\chi = \varphi - \beta$; r is the radius of a turning circle:

$$\dot{\chi} = V\frac{d\chi}{ds}, \qquad r = \frac{V}{\dot{\chi}}, \tag{5}$$

where φ is the yaw angle; β is the sliding angle; s is the angular position of the vehicle mass center along the path.

We note for comparison, that when the θ-stabilization of the zero roll angle was absent in this example, the motion of the model lasted for only 0.3 s, after that the model was wetted. In this case the model roll angle was $\theta = 140°$ at the time $t = 0.3$ s.

5. COURSE θ-CONTROL OF SC-VEHICLE MOTION

The method of θ-control of the SC-vehicle motion on course is based on that the effective angle of the cavitator inclination in the horizontal plane δ_y is changed with varying the SC-vehicle roll angle θ. Hence, projections of vector of the force acting onto the cavitator

are changed too. Indeed, the vehicle roll on the angle θ with preliminary inclination of the cavitator in the diametral plane Ox_1y_1 on the angle δ'_z is equivalent to the cavitator inclination in the two transversely-spaced planes on the angles δ_z and δ_y when $\theta = 0$. The angles δ'_z, θ, δ_z, and δ_y are linked by relations:

$$\operatorname{tg}\delta_z = \frac{\operatorname{tg}\delta'_z}{\cos\theta}, \qquad \operatorname{tg}\delta_y = \frac{\operatorname{tg}\delta'_z}{\sin\theta}. \tag{6}$$

The cavitator inclination on the angle δ_y creates the transversal component of the force F_{nz} [5]. Thus, the cavitator is the real active operating control at the θ-control of the SC-vehicle motion. Therefore, the θ-control is as effective as the δ-control. The required vehicle roll angle $\theta_2 \neq 0$ is attained with the help of the special roll fin *3* (see Fig. 2). To solve a problem of setting and further maintenancing of the required roll angle θ_2, we proposed to use the following algorithm which is analogous to the "reverse of rudder" algorithm when turning surface ships.

1. It is supposed that the roll fin is absent on time interval $0 < t < t_{beg}$ and the model moves without roll: $\theta = 0$, $\omega_x = 0$.

2. The roll fin is deflected on the specified angle δ_{fb} at the time $t = t_{beg}$. After that both the model roll angle θ and the angular velocity ω_x begin to increase.

3. The angle of the roll fin deflection is reversed at the time when $\theta = \theta_1/2$, where θ_1 is the some test roll angle. As a result, the angular velocity ω_x begins to decrease, but the model roll angle θ continues to increase.

4. At the time when $\omega_x = 0$ (in this case the roll angle possesses the value $\theta = \theta_2$) the roll fin angle deflection is set to zero, and then the automatic system of the roll angle θ_2 stabilization (3) is activated.

We note that presence of the metacentric height $h_M > 0$ plays a negative role when using the θ-control of the SC-vehicle motion. Indeed, when the required roll angle θ_2 is stabilized by the automatic control system (3), it must permanently overcome the axial moment (2) tending to set the roll angle $\theta = 0$.

Fig. 5 shows an example of calculating the process of setting and automatic θ-stabilization of the specified roll angle $\theta_2 = 15.0°$ for the SC-vehicle without vertical fins. The calculation was performed for the following parameters: $\theta_1 = 17.6°$, $t_{beg} = 1.0$ s, $u_1 = 0.1$, $u_2 = 0.3$, $\delta_{fb1} = 10.0°$. A graph of the dependence $\delta_{fb}(t)$ is given in Fig. 5a, a graph of corresponding variation of the model roll angle $\theta(t)$ is given in Fig. 5b.

Table 2 gives results of calculation of the average speed of the model course turning $\dot{\chi}$ and the radius of a turning circle r for a number of the roll angles θ. The calculation for each column of Table 2 were performed for fixed magnitude of the roll angle θ on the distance 1.0 km when $x_c = 2.5$ m and $h_M = 0$.

Fig. 6 shows the calculated path configurations of the model mass center (projections onto the horizontal plane) at the θ-control for a number of the regulated roll angles θ_2 on the distance 4.0 km. Comparison with [5] shows that the θ-control of the SC-vehicle motion for its course maneuvering is quite as effective as the δ-control.

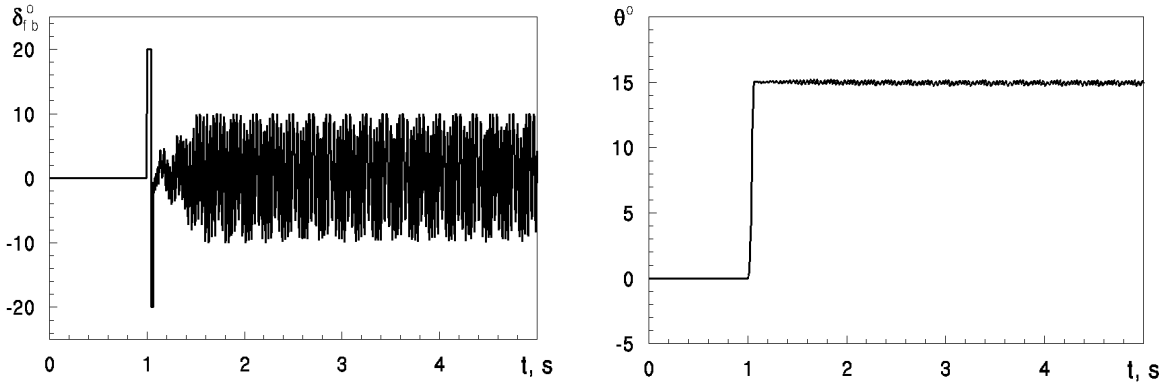

a *b*

Fig. 5. Operation of the automatic system of setting and stabilizing the specified roll angle: *a* — dependence $\delta_{fb}(t)$, *b* — dependence $\theta(t)$

Table 2. Dependence of speed of the SC-model turning and radius of a turning circle on the roll angle

θ,°	0	2.0	5.0	10.0	20.0	30.0	40.0
$\dot{\chi}$,°/s	0	−0.417	−0.743	−0.849	−1.715	−2.711	−3.942
r, km	∞	37.5	16.5	8.09	4.01	2.54	1.74

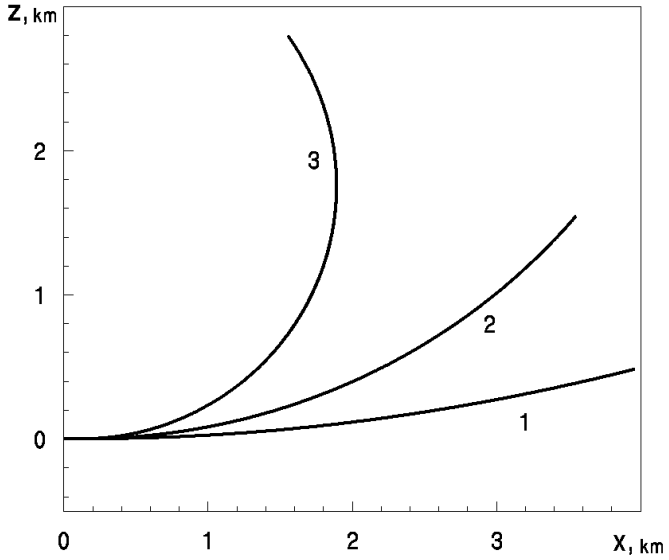

Fig. 6. Path configurations of the θ-controlled SC-model: *1* — $\theta_2 = 6.61°$, *2* — $\theta_2 = 20.85°$, *3* — $\theta_2 = 44.24°$

6. SC-VEHICLE BALANCING WITH FINS

Let us consider the SC-vehicle motion mode, when a pair of horizontal cavity-piercing fins is used for full or partial compensation of the vehicle weight F_g (see Fig. 1b).

The SC-vehicle steady-state longitudinal motion is considered as balanced if a sum of all the forces acting, and a sum of their moments relatively to the model mass center are equal to zero. To determine balanced values of the parameters, we use the numerical method described in work [14]. In this case, the cavitator force $\vec{F}_n$, the horizontal fin force $\vec{F}_f$, the planing force $\vec{F}_s$, the propulsor thrust $\vec{F}_{pr}$, and the body weight F_g act onto the vehicle. A set of equations of the SC-vehicle balance in projections onto the body coordinates has the form:

$$\begin{aligned} F_{nx} + F_{sx} + F_{fx} + F_g \sin\psi - F_{pr}\cos\eta_z = 0, \\ F_{ny} + F_{sy} + F_{fy} + F_g \cos\psi - F_{pr}\sin\eta_z = 0, \\ M_{nz} + M_{sz} + M_{fz} + F_{pr}\sin\eta_z(L - x_c) = 0, \end{aligned} \tag{7}$$

where η_z is the thrust vector deflection; $M_{nz} = -F_{ny}x_c$; $M_{sz} = F_{sy}(x_s - x_c)$; $M_{fz} = F_{fy}(x_f - x_c)$; x_s, x_f are the points of application of the forces $\vec{F}_s$ and $\vec{F}_f$, respectively. Eliminating F_{pr} from equations (7), we obtain a set of two equations with four unknowns:

$$F_1(\delta_z, \delta_{fh}, \eta_z, \psi) = 0, \qquad F_2(\delta_z, \delta_{fh}, \eta_z, \psi) = 0. \tag{8}$$

Fixing any two of the four angles δ_z, δ_{fh}, η_z, ψ, one can determine from it the balanced values of two other angles with the help of the Newton's iteration algorithm [14].

Fig. 7 shows character of influence of both the mass center position $\bar{x}_c = x_c/L$ and the horizontal fin position $\bar{x}_{fh} = x_{fh}/L$ onto the balanced parameters of the model with the specified mass m. Graphs of dependence of the balanced values δ_z and δ_{fh} on $\bar{x}_c$ are given in Fig. 7a for fixed $\eta_z = 0$, $\psi = 0$, $\bar{x}_{fh} = 0.8$. Graphs of dependence of the balanced values δ_z and δ_{fh} on $\bar{x}_{fh}$ are given in Fig. 7b for fixed $\eta_z = 0$, $\psi = 0$, $\bar{x}_c = 0.5$.

We note that the problem of balancing the SC-vehicle with horizontal fins may not have a solution for the specified vehicle mass m and admissible ranges of varying the parameters

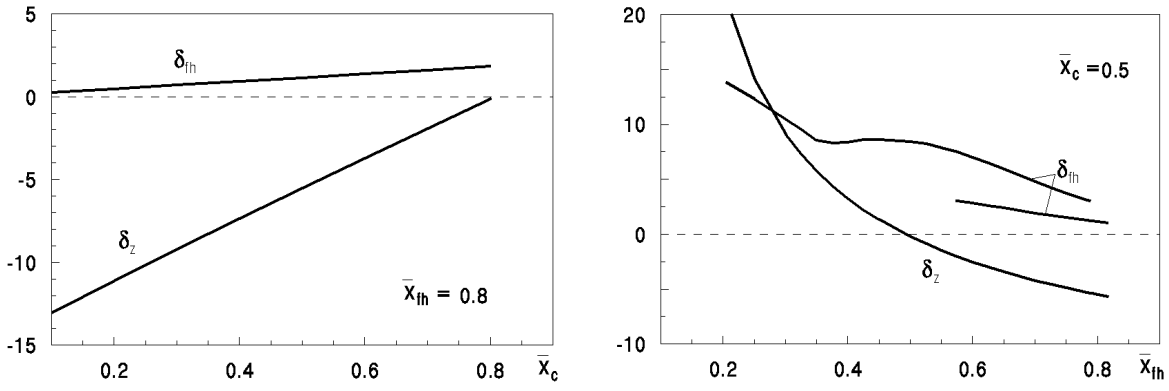

a b

Fig. 7. Balanced angles δ_z and δ_{fh} when $\eta_z = 0$, $\psi = 0$:
a — dependence on $\bar{x}_c$, b — dependence on $\bar{x}_{fh}$

x_c, x_{fh}, δ_z, δ_{fh}, η_z, ψ. Also, it may have an ambiguous solution caused by nonmonotonic dependence $c_{fy}(\delta_{fh})$ for SC-fins having a wedge-shaped cross section [17]. So, in the case of Fig. 7b the SC-model may not be balanced when $\bar{x}_{fh} < 0.204$, and it has two balanced values δ_{fh} for each $0.572 < \bar{x}_{fh} < 0.789$.

7. DYNAMICS OF SC-VEHICLE BALANCED WITH FINS

Computer simulation allows a difference in dynamic behavior of the SC-vehicle to be shown, which was balanced in the planing in a cavity mode (see Fig. 1a), in the planing avoidance mode (see Fig. 1b), and in the combined mode.

As is known, the longitudinal motion of the SC-vehicle without fins in the planing in a cavity mode is unstable "in the small". In this case the stability loss occurs in a "soft" oscillatory manner, and increasing the model angular oscillation amplitude is limited by interaction between the model and the cavity walls. In this case to prevent increasing the vehicle mass center deflection from the horizontal path y one should apply the automatic δ-stabilization of motion on depth, which makes the motion global stable [2, 6].

On the contrary, computer simulation showed that the motion of the SC-model with the horizontal fins in the planing avoidance mode is stable "in the small". In this case an allowable range of deflections of the pitch angle ψ from its balanced value exists when the solution fast tends to the balanced one.

In the combined mode, i. e., if both the horizontal fins and the model planing in a cavity are presented, computer simulation shows the complex SC-model dynamics which essentially depends on the starting values of the parameters. In this case, it turned out that the balanced pitch angle ψ and, hence, the model tail edge immersion in water h have a basic importance. As calculation showed, the horizontal fins may play a damping role for relatively great value of h, suppressing the motion instability "in the small".

Fig. 8 gives a comparison of graphs of dependence $\psi(\bar{s})$ in the combined mode of the SC-model motion for two starting values $\psi_0 = 0.4$ and $\psi_0 = 0.5$. The graphs have the following nomenclature: $\bar{s} = s/L$ is the distance along the path; $\bar{y} = y/L$ is the deflection of the model mass center from the horizontal path; magnitudes of the angle ψ are plotted in degrees. It

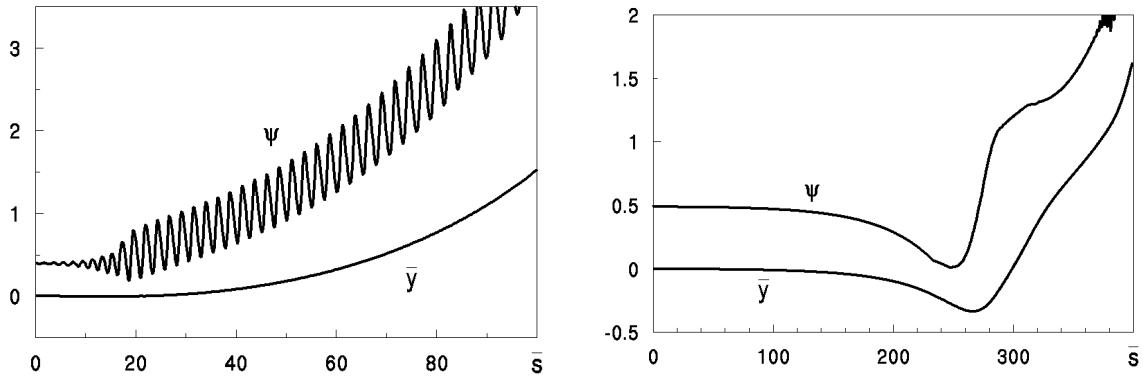

a b

Fig. 8. Dynamics of the SC-model balanced in the combined mode:
a — $\psi_0 = 0.4$, b — $\psi_0 = 0.5$

Table 3. Effect of starting balancing on maneuverability of the f-controlled SC-model

No.	1	2	3	4	5	6	7	8
ψ_0,°	0.371	0	0.1	0.2	0.3	0.4	0.5	0.6
h_0, mm	1.07					3.76	12.98	23.23
δ_{fh},°		1.130	0.930	0.730	0.530	−4.123	−9.750	−13.072
$\dot{\chi}$, °/s	−4.942	−10.693	−8.468	−5.307	−5.076	−3.085	−3.034	−2.764
r, km	1.383	0.642	0.810	1.291	1.348	2.208	2.254	2.433

was accepted in the calculation that $\bar{x}_c = 0.5$, $\bar{x}_{fh} = 0.8$.

In case Fig. 8a the model was balanced at the following parameters: $\psi = 0.4$, $\eta_z = 0$, $\delta_z = -5.948°$, $\delta_{fh} = -4.138°$, $F_{pr} = 23.896$ KN. As can be seen, in this case the dynamic behavior of the SC-model is quite similar to the case of motion in the planing in a cavity mode without fins [6]. After loss of stability "in the small", the model performs angular oscillation with the frequency 7.8 Hz. It reaches the free water surface after 5.1 s.

In case Fig. 8b the model was balanced at the following parameters: $\psi = 0.5$, $\eta_z = 0$, $\delta_z = -5.642°$, $\delta_{fh} = -9.756°$, $F_{pr} = 25.656$ KN. As can be seen, in this case high-frequency angular oscillation of the model does not arise. However, after a long time interval the motion loses the global stability. In both the cases, using the depth δ-stabilization of motion [6] makes it stable in global.

A question about the effect of starting balancing the f-controlled SC-vehicle on its course maneuverability is of interest. Table 3 gives results of calculation of the SC-model motion after distance 1 km when $\delta_{fv} = -5°$ for a number of the starting balanced pitch angles ψ_0. The fin parameters are given in Table 1. When calculation both the roll θ-stabilization of motion (3) and the depth δ-stabilization of motion [6] were activated.

In Table 3, the balanced values of both the model aft edge immersion in water h_0 and the horizontal fin deflection angle δ_{fh}, average values of the model turning speed $\dot{\chi}$, and average values of the radius of a turning circle r are given. The column 1 of the table corresponds to the case of the planing in a cavity mode without horizontal fins. The columns 2 to 5 correspond to the case of starting balancing in the planing avoidance mode. The columns 6 to 8 correspond to the case of starting balancing in the combined mode.

As can be seen, the SC-vehicle course maneuverability is maximal at the starting balancing in the planing avoidance mode, but it dramatically deteriorates at the starting balancing in the combined mode.

8. CONCLUSIONS

A method of active roll stabilization of the SC-vehicle motion with the help of both the bottom roll fin and the automatic error-closing control system has been devised. It was shown that the stabilization of the zero roll angle is necessary when the f-controlled SC-vehicle course maneuvering. The same method can be used for the course θ-control of the SC-vehicle motion by setting the specified roll angle θ_2 and the further automatic θ-stabilization of this roll angle.

Since the active operating control at the θ-control of the SC-vehicle motion is the cavitator, the θ-control has the same advantages and limitations as the δ-control [16]. As a result of the comparative analysis of the advantages and disadvantages of each of the four methods of course controlling the SC-vehicle motion, it can be concluded that the proposed θ-control method is optimal within its efficiency.

A method of determination of the balanced motion parameters (balancing) of the SC-vehicle in the case, when a pair of identical horizontal cavity-piercing fins is used for full or partial compensation of the vehicle weight, has been devised.

It was shown that the longitudinal motion of the balanced with the horizontal fins SC-vehicle in the planing avoidance mode is stable "in the small". In the combined mode, i. e., if both the horizontal fins and the planing of the model body in a cavity are presented, the computer simulation shows the complex SC-vehicle dynamic behaviour which essentially depends on the starting value of the pitch angle ψ. For relatively big values of ψ the horizontal fins may play a damping role, suppressing the SC-vehicle motion instability "in the small". However, after a long time interval motion loses the global stability.

In all the examined cases, activation of the automatic depth δ-stabilization [6] makes the SC-vehicle motion stable in global. It was shown that the f-controlled SC-vehicle course maneuverability is maximal at the starting balancing in the planing avoidance mode, but it dramatically deteriorates at the starting balancing in the combined mode.

ЛІТЕРАТУРА

[1] Логвинович Г. В. Гидродинамика течений со свободными границами. — Киев : Наукова думка, 1969. — С. 215.

[2] Dzielski J., Kurdila A. A benchmark control problem for supercavitating vehicles and an initial investigation of solution // Journal of Vibration and Control. — 2003. — Vol. 9, no. 7. — P. 791–804.

[3] Control strategies for supercavitating vehicles / I. N. Kirschner, D. C. Kring, A. W. Stokes et al. // Journal of Vibration and Control. — 2002. — Vol. 8, no. 2. — P. 219–242.

[4] Trajectory optimization strategies for supercavitating underwater vehicles / M. Ruzzene, R. Kamada, C. L. Bottasso, F. Scorcelletti // Journal of Vibration and Control. — 2008. — Vol. 14, no. 5. — P. 611–644.

[5] Савченко Ю. Н., Семененко В. Н. О маневренности по курсу подводных суперкавитирующих аппаратов // Прикладна гідромеханіка. — 2011. — Т. 13(85), № 1. — С. 43–50.

[6] Semenenko V. N., Naumova Y. I. Study of the supercavitating body dynamics // Supercavitation: Advances and perspectives. — Berlin and Heidelberg : Springer-Verlag, 2012. — P. 147–176.

[7] Семененко В. Н. Расчет пространственного движения суперкавитирующих аппаратов // Прикладна гідромеханіка. — 2012. — Т. 14(86), № 4. — С. 59–64.

[8] Semenenko V. N. Prediction of supercavitating vehicle maneuvering // Proceedings of the 11th International Scientific School "High Speed Hydrodynamics and Shipbuilding (HSH-2013)". — Cheboksary, Russian Federation, 2013.

[9] Sanabria D. E., Balas G. J., Arndt R. E. A. Planing avoidance control for supercavitating vehicles // 2014 American Control Conference. — Portland, OR, 2014. — P. 4979–4984.

[10] Grumondz V. T., Korzhov D. N. On stability of steady motion of a high-speed underwater vehicle with ring-like stern wing // Proceedings of the International Conference on Underwater Technologies (SubSeeTech 2014). — St. Petersburg, Russian Federation, 2014.

[11] Kim S., Kim N. Studies on planing avoidance control for a ventilated supercavitating vehicle // Journal of the Society of Naval Architects of Korea. — 2016. — Vol. 53, no. 3. — P. 201–209.

[12] Логвинович Г. В., Серебряков В. В. О методах расчета формы тонких осесимметричных каверн // Гидромеханика. — 1975. — С. 47–54.

[13] Semenenko V. N. Artificial cavitation. Physics and calculations // Supercavitating Flows. — RTO/NATO, 2002. — P. 11(1–33).

[14] Semenenko V. N., Naumova O. I. Dynamics of a partially cavitating underwater vehicle // Гідродинаміка і акустика. — 2018. — Т. 1(91), № 1. — С. 70–84.

[15] Paryshev E. V. On unsteady planning of a body over liquid curvilinear surface // Proceedings of the 2nd International Summer Scientific School "High Speed Hydrodynamics". — Cheboksary, Russian Federation, 2004. — P. 175–178.

[16] Савченко Ю. Н., Семененко В. Н., Савченко Г. Ю. Особенности маневрирования при суперкавитационном обтекании // Прикладна гідромеханіка. — 2016. — Т. 18(90), № 1. — С. 79–82.

[17] Savchenko Y. N., Semenenko V. N. Special features of supercavitating flow around polygonal contours // International Journal of Fluid Mechanics Research. — 2001. — Vol. 28, no. 5. — P. 660–672.

[18] Savchenko Y. N. Control of supercavitation flow and stability of supercavitating motion of bodies // Supercavitating Flows. — RTO/NATO, 2002. — P. 14(1–29).

REFERENCES

[1] G. V. Logvinovich, *Hydrodynamics of flows with free boundaries.* Kyiv: Naukova Dumka, 1969.

[2] J. Dzielski and A. Kurdila, "A benchmark control problem for supercavitating vehicles and an initial investigation of solution," *Journal of Vibration and Control*, vol. 9, no. 7, pp. 791–804, 2003.

[3] I. N. Kirschner, D. C. Kring, A. W. Stokes, N. E. Fine, and J. J. S. Uhlman, "Control strategies for supercavitating vehicles," *Journal of Vibration and Control*, vol. 8, no. 2, pp. 219–242, 2002.

[4] M. Ruzzene, R. Kamada, C. L. Bottasso, and F. Scorcelletti, "Trajectory optimization strategies for supercavitating underwater vehicles," *Journal of Vibration and Control*, vol. 14, no. 5, pp. 611–644, 2008.

[5] Y. N. Savchenko and V. N. Semenenko, "On the course maneuvering of underwater supercavitating vehicles," *Applied Hydromechanics*, vol. 13(85), no. 1, pp. 43–50, 2011.

[6] V. N. Semenenko and Y. I. Naumova, "Study of the supercavitating body dynamics," in *Supercavitation: Advances and perspectives*, pp. 147–176, Berlin and Heidelberg: Springer-Verlag, 2012.

[7] V. N. Semenenko, "Calculation of 3D motion of supercavitating vehicles," *Applied Hydromechanics*, vol. 14(86), no. 4, pp. 59–64, 2012.

[8] V. N. Semenenko, "Prediction of supercavitating vehicle maneuvering," in *Proceedings of the 11th International Scientific School "High Speed Hydrodynamics and Shipbuilding (HSH-2013)"*, (Cheboksary, Russian Federation), 2013.

[9] D. E. Sanabria, G. J. Balas, and R. E. A. Arndt, "Planing avoidance control for supercavitating vehicles," in *2014 American Control Conference*, (Portland, OR), pp. 4979–4984, 2014.

[10] V. T. Grumondz and D. N. Korzhov, "On stability of steady motion of a high-speed underwater vehicle with ring-like stern wing," in *Proceedings of the International Conference on Underwater Technologies (SubSeeTech 2014)*, (St. Petersburg, Russian Federation), 2014.

[11] S. Kim and N. Kim, "Studies on planing avoidance control for a ventilated supercavitating vehicle," *Journal of the Society of Naval Architects of Korea*, vol. 53, no. 3, pp. 201–209, 2016.

[12] G. V. Logvinovich and V. V. Serebryakov, "On the methods of calculating a shape of the slender axisymmetric cavities," *Hydromechanics*, vol. 32, pp. 47–54, 1975.

[13] V. N. Semenenko, "Artificial cavitation. Physics and calculations," in *Supercavitating Flows*, pp. 11(1–33), RTO/NATO, 2002.

[14] V. N. Semenenko and O. I. Naumova, "Dynamics of a partially cavitating underwater vehicle," *Hydrodynamics and Acoustics*, vol. 1(91), no. 1, pp. 70–84, 2018.

[15] E. V. Paryshev, "On unsteady planning of a body over liquid curvilinear surface," in *Proceedings of the 2nd International Summer Scientific School "High Speed Hydrodynamics"*, (Cheboksary, Russian Federation), pp. 175–178, 2004.

[16] Y. N. Savchenko, V. N. Semenenko, and G. Y. Savchenko, "Features of manoeuvring at the supercavitation flowing around," *Applied Hydromechanics*, vol. 18(90), no. 1, pp. 79–82, 2016.

[17] Y. N. Savchenko and V. N. Semenenko, "Special features of supercavitating flow around polygonal contours," *International Journal of Fluid Mechanics Research*, vol. 28, no. 5, pp. 660–672, 2001.

[18] Y. N. Savchenko, "Control of supercavitation flow and stability of supercavitating motion of bodies," in *Supercavitating Flows*, pp. 14(1–29), RTO/NATO, 2002.

В. М. Семененко, О. І. Наумова

Деякі способи застосування гідродинамічного руля для суперкавітуючих підводних апаратів

Розглянуто два нетрадиційні способи застосування гідродинамічних рулів при русі високошвидкісних підводних суперкавітуючих апаратів. Розроблено метод активної стабілізації руху суперкавітуючого апарату за креном і метод керування його рухом за курсом шляхом регулювання кута крену за допомогою спеціального руля крену й автоматичної системи керування зі зворотним зв'язком. Наведено приклади комп'ютерного моделювання маневрування суперкавітуючого апарату за курсом при керуванні за допомогою вертикальних гідродинамічних рулів зі стабілізацією нульового кута крену і шляхом регулювання кута крену. Розроблено метод знаходження рівноважних значень параметрів руху (балансування) суперкавітуючого апарату у випадку, коли для повної чи часткової компенсації його ваги використовується пара однакових горизонтальних рулів, які проникають з каверни у воду. Наведено приклади комп'ютерного моделювання руху суперкавітуючого апарату з горизонтальними рулями в режимі без глісування і в змішаному режимі. Показано, що усталений поздовжній рух збалансованого суперкавітуючого апарату без глісування, на відміну від його руху в режимі глісування в каверні, є стійким «в малому». Встановлено, що в змішаному режимі руху горизонтальні рулі можуть грати демпфуючу роль, пригнічуючи нестійкість руху апарату «в малому», однак на великому інтервалі часу рух втрачає стійкість в цілому. Моделювання показало, що застосування автоматичної стабілізації руху по глибині у всіх розглянутих випадках робить його стійким в цілому. Показано також, що курсова маневреність такого апарату при керуванні за допомогою вертикальних рулів максимальна при початковому балансуванні в режимі без глісування, але різко погіршується при початковому балансуванні в змішаному режимі.

КЛЮЧОВІ СЛОВА: суперкавітуючий апарат, керування, маневрування, рулі, крен, комп'ютерне моделювання

В. Н. Семененко, О. И. Наумова

Некоторые способы применения гидродинамического руля для суперкавитирующих подводных аппаратов

Рассмотрены два нетрадиционных способа применения гидродинамических рулей при движении высокоскоростных подводных суперкавитирующих аппаратов. Разработан метод активной стабилизации движения суперкавитирующего аппарата

по крену и метод управления его движением по курсу путем регулирования угла крена с помощью специального руля крена и автоматической системы управления с обратной связью. Приведены примеры компьютерного моделирования маневрирования суперкавитирующего аппарата по курсу при управлении с помощью вертикальных гидродинамических рулей со стабилизацией нулевого угла крена и путем регулирования угла крена. Разработан метод нахождения равновесных значений параметров движения (балансировки) суперкавитирующего аппарата в случае, когда для полной или частичной компенсации его веса используется пара одинаковых горизонтальных рулей, проникающих из каверны в воду. Приведены примеры компьютерного моделирования движения суперкавитирующего аппарата с горизонтальными рулями в режиме без глиссирования и в смешанном режиме. Показано, что установившееся продольное движение сбалансированного суперкавитирующего аппарата без глиссирования, в отличие от его движения в режиме глиссирования в каверне, является устойчивым «в малом». Установлено, что в смешанном режиме движения горизонтальные рули могут играть демпфирующую роль, подавляя неустойчивость движения аппарата «в малом», однако на большом интервале времени движение теряет устойчивость в целом. Моделирование показало, что применение автоматической стабилизации движения по глубине во всех рассмотренных случаях делает его устойчивым в целом. Показано также, что курсовая маневренность такого аппарата при управлении с помощью вертикальных рулей максимальна при начальной балансировке в режиме без глиссирования, но резко ухудшается при начальной балансировке в смешанном режиме.

КЛЮЧЕВЫЕ СЛОВА: суперкавитирующий аппарат, управление, маневрирование, рули, крен, компьютерное моделирование